Iran J Sci Technol Trans Electr Eng (2019) 43:153–165
https://doi.org/10.1007/s40998-018-0066-4

RESEARCH PAPER

# A Fuzzy-Based Controller of a Modified Six-Phase Induction Motor Driving a Pumping System

**Mohamed I. Abdelwanis**[1] · **Ragab A. El-Sehiemy**[1]

Received: 7 May 2017 / Accepted: 11 May 2018 / Published online: 9 July 2018


**Abstract**

This study presents the implementation and analysis of the modified six-phase induction motor (IM) that drives a centrifugal pumping system. The three-phase IM is modified to operate as a six-phase IM to enhance the torque pulsation and to increase the motor reliability. Dynamic models of six-phase IM are derived. A fuzzy-based procedure for fine-tuning of the PID controller parameters is proposed in order to sustain the motor speed at the predefined reference values. Added to that, a six-phase low-pass filter is designed to eliminate the undesirable harmonics contents. An optimized PID controller accomplished with a scalar V/f closed-loop six-phase induction motor control is presented and its simulation results are discussed. Pulse width modulation (PWM)-based simulation studies were employed for six-phase induction motor using MATLAB/SIMULINK software. The simulation results show that the PWM inverter reduces the THD for current and voltage waveforms and the overall performance of the modified six-phase IM is enhanced compared with the equivalent three-phase induction motor.

**Keywords** Six-phase induction motor · Sensorless speed · Centrifugal pump · PWM · Harmonic distortion

**List of symbols**

| | |
|---|---|
| $J$ | Inertia of the system, kg m$^2$ |
| $B$ | Friction |
| $H$ | Total pumping head, m |
| $Q$ | Flow rate, m$^3$/h |
| $P_h$ | Hydraulic power of pump, W |
| $R_s$, $R_r$ | Stator and rotor resistances, Ω |
| $\omega$ | Angular speed of arbitrary frame |
| $\omega_r$ | Angular speed of rotor frame |
| $I_{ds}$, $I_{qs}$ | Direct and quadrature axis stator current, A |
| $L_{ls}$, $L_{lr}$ | Stator and rotor inductance of motor, respectively, H |
| $L_m$ | Magnetization inductance, H |
| $P$ | Number of pole pairs |
| $T_e$ | Electromagnetic torque of the motor, N m |
| $T_p$ | Constant torque of the pump, N m |
| $V_{ds}$, $V_{qs}$ | Direct and quadrature component of stator voltage, V |
| $V$ | Terminal voltage of the array, V |
| $\psi_{ds}$, $\psi_{qs}$ | Direct and quadrature component of stator flux |

✉ Mohamed I. Abdelwanis
mohamed.soliman4@eng.kfs.edu.eg

Ragab A. El-Sehiemy
elsehiemy@eng.kfs.edu.eg

[1] Intelligent Systems Research Group (ISRG), Electrical Engineering Department, Faculty of Engineering, Kafrelsheikh University, Kafrelsheikh, Egypt

## 1 Introduction

### 1.1 Motivation

Generally, the field of multiphase variable speed motors' drives has knowledgeable and extensive development of many motivating progresses that were reported in the literature (Levi et al. 2007). The dual three-phase IM connection, the typical construction of six phases IM, having two winding sets placed in stator shifted by 60 electrical degrees. The integration of dual three-phase IM for industrial applications grants numerous benefits over the conventional three-phase IM. These benefits are enhanced reliability, reduced magnetic flux harmonic, minimized torque pulsations, and reduced size of the static power converter (Lyra and Lipo 2002). Added to these benefits, another advantage of multiphase IM drives over conventional three-phase drives is the ability of continuous system operation at abnormal operating modes after the excitation loss of one or more stator phases (Kiani-Nezhad et al. 2008; Fnaiech et al. 2010). In addition, the dual three-phase IM generates higher operational torque compared with three-phase IM. The higher operational torque characteristic makes IM suitable in high power and/or high current applications, such as electric hybrid vehicles, ship propulsion, and aerospace applications. The six-phase IM is one of the best acceptable alternatives in industry application when high power industry applications are found. The recent trend in high power applications is to replace six-phase synchronous motor by six-phase IM as the latter weight is lower than six-phase synchronous motors at the same rating (Taheri et al. 2012; Renukadevi and Rajambal 2012; Nanoty and Chudasama 2012a, 2013).

## 1.2 Literature Review

There have been several attempts to develop multiphase IM which are characterized with high degree of reliability over three-phase IM (Lyra and Lipo 2002; Nanoty and Chudasama 2012b; Barrero and Duran 2016a, b; Kang et al. 2009). The six-phase IM windings are placed in the same stator of three-phase IM. The current per phase in the six-phase IM is reduced. Therefore, total power rating of the system is theoretically doubled as each set of three-phase stator winding is excited by a three-phase inverter. In 1969, Ward and Harner for the first time have presented the previous investigation of an inverter-fed multiphase IM and suggested that the pulsation of torque can be minimized by maximizing the phases number of stator (Sriram Pavan Kumar and Kalyan Chakravarthi 2016; Kundrotas et al. 2011).

A six-phase motor needs an input supply of six-phase voltage source inverter (VSI). To achieve the better output voltage for three-phase inverters, the sinusoidal pulse width modulation (SPWM) method, space vector pulse width modulation (SVPWM), harmonic injection method, and offset injection method are extensively studied. The SPWM inverters are more flexible and easy to carry out. However, the waveforms of output voltage contain more harmonics resulting in reduced efficiency and fundamental component (Levi et al. 2007). The difficulty involved in the SVPWM inverter is increased for higher number of phases. A simple and better switching technique is needed for multiphase voltage source inverter which would overcome the complexity involved with higher number of phases (Renukadevi and Rajambal 2013; Lega et al. 2010).

In Renukadevi and Rajambal (2013), compared with their three-phase counterparts, multiphase machines with phase number $n \geq 5$ have several advantages as lower torque pulsation, higher power density, better fault tolerance, etc. due to these advantages and the increasing demands on higher phases machines. In Kang et al. (2009), the magnetic motive force of stator is kept constant to produce smooth torque after one or more phases are open circuit. The nine-phase IM was designed for four-pole operation and it can also be applied to operate in three-phase, 12-pole configuration by rearranging the stator winding connections using the pole modulation technique of phase (Gautam et al. 2012). In Pant (2000), the dynamic and steady-state behaviour of a multiphase IM during faulty condition was analysed.

In Sciuller et al. (2006), analytical and finite element methods were developed for seven-phase axial-flux double-rotor permanent magnet synchronous machine. In Singh (2002), the multiphase IM drive research that was presented with concentrating on the analytical and technical attention was addressed towards practical realization of the merits of this new technology. Kim et al. (2003) improve the saliency of EMF-based methods by using feed-forward observer to estimate the rotor indication signals. The lagging properties of the state filter can be eliminated. The outcome is zero-phase lag assessment of the motion states.

In the literature, Volts/Hz control, flux vector, and vector control methods are developed for controlling the induction motors operation. The first method aims to maintain constant motor magnetic flux, and it is valid for control of an induction motor in the gradually varying and expectable load applications. The flux vector control method was developed to control the magnitude of the ac voltage, and vector. The third method is modifying the amplitude, frequency, and phase of the drive voltage. The aim is to generate modified three-phase voltage to control the stator current which in turn controls the rotor flux vector and current independently. The position of flux vector can be found by two ways, direct and indirect methods. The direct method uses sensors put in stator which increase the cost, size, and harmonics of IM. Hence, using the indirect method, this flux vector can be found by parameters and modelling equations of machine governing its performance. Hence, vector control method has gained importance (Abdelwanis et al. 2015; Abdelwanis and Selim 2015; Fatemi et al. 2014).

Developing the converter side for improving the performance of six-phase IM is presented in Azeddine and Ghalem (2010). In Nabi et al. (2011), a new structure is proposed for vector control of symmetrical six-phase IM based on the usage of three current sensors. The performance analysis of six-phase IM is developed in Mandal (2015). A modified multiphase IM with high starting current was suggested in Nagaraj et al. (2014).

Fuzzy logic is an efficient tool that is able to enhance the electrical apparatus in power systems operation. Numerous applications of fuzzy controller are examined in El-Sehiemy et al. (2017), Elhosseini et al. (2017), El-Ela et al. (2005), El-Sehiemy et al. (2013), Abou et al. (2010), Kudinov et al. (2017), and El-Sehiemy et al. (2015). Developing the fuzzy logic and sliding mode controllers to enhance the operation by achieving high-accuracy positioning of six-phase IM is presented in Fnaiech et al. (2010).The parameters of PID controller were scheduled using fuzzy logic tuner to enhance overall optimal system performance specified by a cost function (El-Sehiemy et al. 2015; Han et al. 2003; Xu et al. 2006; Ho and Yeh 2010; Xia et al. 2010; Zhao and Yuan 2011; Kumar and Daya 2013).

### 1.3 Paper Innovation

The main contribution of the current paper can be summarized as follows:

- The three-phase induction motor is modified to six-phase induction motor to enhance torque pulsation and the motor reliability.
- The dynamic models of six-phase IM are derived.
- This paper provides the modelling and analysis of PID and fuzzy PID controllers applied to the modified six-phase IM that drives variable speed centrifugal pump system.
- A fuzzy-based tuned PID controller is proposed to sustain the motor speed at the predefined reference values that were correlated to the operating condition.
- A six-phase low-pass filter is designed to eliminate the undesirable harmonics contents.
- A scalar V/f closed-loop six-phase induction motor control is presented and its simulation results are discussed.

### 1.4 Paper Organization

The rest sections of this paper are organized as follows: In Sect. 2, the modelling of PWM for six-phase inverter is analysed. Six-phase squirrel induction motor model is presented in Sect. 3. The proposed control strategy involving the speed estimation and the closed-loop scheme is presented in Sect. 4. Section 5 analyses the simulation and practical results. Section 6 concludes the output findings of the paper.

## 2 Modelling of Pulse Width-Modulated (PWM) Six-Phase Inverter

The PWM techniques and three-phase inverter are able to produce a variable V/F sinusoidal waveform to control the speed of an IM. A typical six-phase inverter is shown in Fig. 1a, Fatemi et al. (2014). The model of six-phase inverter is shown in Fig. 1b.

The analysis equations according to KVL are presented as (Fatemi et al. 2014):

$$\begin{cases} v_{ao} = v_{an} + v_{no} \\ v_{bo} = v_{bn} + v_{no} \\ v_{co} = v_{cn} + v_{no} \\ v_{do} = v_{dn} + v_{no} \\ v_{eo} = v_{en} + v_{no} \\ v_{fo} = v_{fn} + v_{no} \end{cases}. \tag{1}$$

Therefore, $v_{no}$ is computed from Eq. (2) as:

$$v_{no} = 1/6(v_{ao} + v_{bo} + v_{co} + v_{do} + v_{eo} + v_{fo}). \tag{2}$$

Combining Eqs. (1) and (2) leads to:

$$\begin{bmatrix} v_{an} \\ v_{bn} \\ v_{cn} \\ v_{dn} \\ v_{en} \\ v_{fn} \end{bmatrix} = \frac{1}{6}\begin{bmatrix} 5 & -1 & -1 & -1 & -1 & -1 \\ -1 & 5 & -1 & -1 & -1 & -1 \\ -1 & -1 & 5 & -1 & -1 & -1 \\ -1 & -1 & -1 & 5 & -1 & -1 \\ -1 & -1 & -1 & -1 & 5 & -1 \\ -1 & -1 & -1 & -1 & -1 & 5 \end{bmatrix}\begin{bmatrix} v_{ao} \\ v_{bo} \\ v_{co} \\ v_{do} \\ v_{eo} \\ v_{fo} \end{bmatrix}. \tag{3}$$

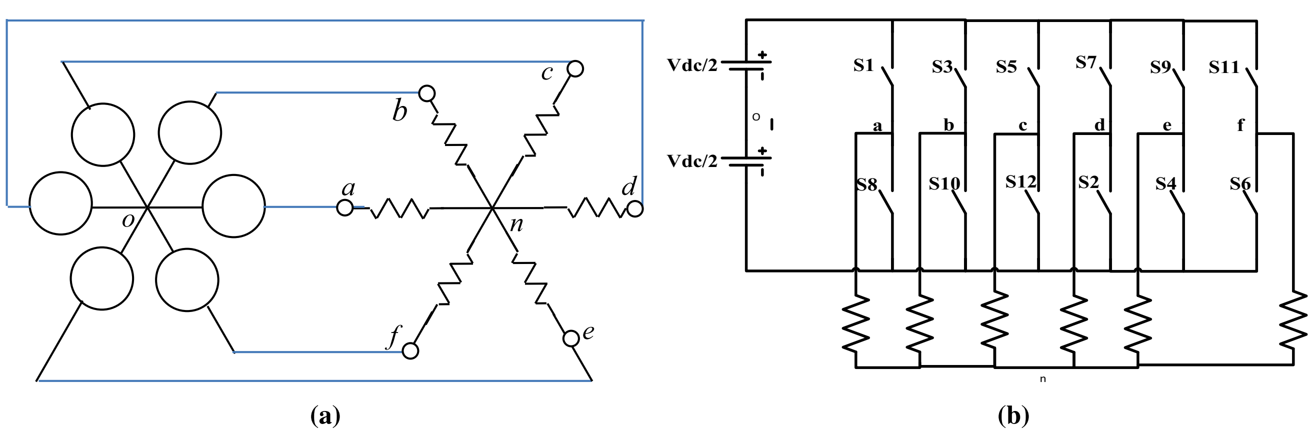


Fig. 1 Six-phase inverter circuit. **a** Primary six-phase inverter, **b** modified six-phase inverter circuit

## 3 Six-Phase Squirrel Induction Motor Model

The six-phase IM stator and rotor windings in space are shown in Fig. 2. The machine is represented in the $q$–$d$-axis reference frame to avoid time-change inductances in the terminal voltage. The $q$–$d$-axis reference frame is fixed in the rotor, which rotates at $\omega_r$ (Azeddine and Ghalem 2010; Nabi et al. 2011; Mandal 2015; Nagaraj et al. 2014).

The sinusoidal voltages of six-phase induction motor are expressed as:

$$\begin{cases} v_{as} = V_m \sin(\omega t) \\ v_{bs} = V_m \sin\left(\omega t - \frac{\pi}{3}\right) \\ v_{cs} = V_m \sin\left(\omega t - \frac{2\pi}{3}\right) \\ v_{ds} = V_m \sin(\omega t - \pi) \\ v_{es} = V_m \sin\left(\omega t - \frac{4\pi}{3}\right) \\ v_{fs} = V_m \sin\left(\omega t - \frac{5\pi}{3}\right) \end{cases}. \tag{4}$$

The voltage decomposition $d$–$q$ axes of six-phase IM can be reformulated as:

$$V_q = \frac{2}{6}\left[\sum_{k=1}^{6} v_k \cos\left(\theta - \frac{(k-1)\pi}{6}\right)\right] \tag{5}$$

$$V_d = \frac{2}{6}\left[\sum_{k=1}^{6} v_k \sin\left(\theta - \frac{(k-1)\pi}{6}\right)\right]. \tag{6}$$

The $q$-axis flux and current component in stator and rotor are represented as:

$$\psi_{qs} = \frac{1}{s}\left[V_{qs} - R_s i_{qs} - \omega_e \psi_{ds}\right] \tag{7}$$

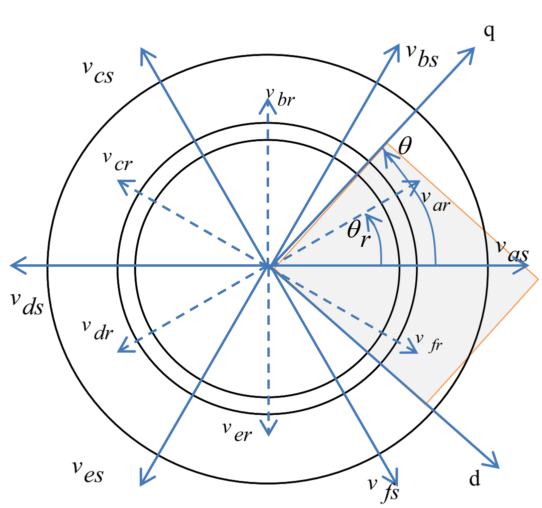


**Fig. 2** Relationship between abs arbitrary dq0

$$i_{qs} = \frac{1}{L_s}\left[\psi_{qs} - L_m i_{qr}\right] \tag{8}$$

$$\psi_{qr} = \frac{1}{s}\left[-R_r i_{qr} + (\omega_r - \omega_e)\psi_{dr}\right] \tag{9}$$

$$i_{qr} = \frac{1}{L_r}\left[\psi_{qr} - L_m i_{qs}\right] \tag{10}$$

$d$-axis flux and current in stator and rotor

$$\psi_{ds} = \frac{1}{s}\left[V_{ds} - R_s i_{ds} - \omega_e \psi_{qs}\right] \tag{11}$$

$$i_{ds} = \frac{1}{L_s}\left[\psi_{ds} - L_m i_{dr}\right] \tag{12}$$

$$\psi_{dr} = \frac{1}{s}\left[-R_r i_{dr} + (\omega_e - \omega_r)\psi_{qr}\right] \tag{13}$$

$$i_{dr} = \frac{1}{L_r}\left[\psi_{qr} - L_m i_{ds}\right]. \tag{14}$$

The torque and speed are written as follows:

$$T_e = \frac{6}{2}\frac{p}{2}\left[\psi_{ds} i_{qs} - \psi_{qs} i_{ds}\right] \tag{15}$$

$$\omega_r = \frac{p}{2}\frac{1}{s}\left[\frac{1}{J}\left(T_e - T_L - D\frac{2}{p}\omega_r\right)\right] \tag{16}$$

$$n_r = \frac{2}{p}\frac{60}{2\pi}\omega_r \tag{17}$$

$$\omega_e = \theta = 0. \tag{18}$$

The electric torque expression is:

$$T_e = \frac{3}{2}\frac{p}{2}\left[\lambda_{ds} I_{qs} - \lambda_{qs} I_{ds}\right]. \tag{19}$$

The mechanical balance equation of motor is:

$$T_e = T_l + J\frac{d\omega_m}{dt} + B\omega. \tag{20}$$

The performance curve of centrifugal pump is modelled as (Renukadevi and Rajambal 2013):

$$H = a_0\omega_r^2 + a_1\omega_r Q + a_2 Q^2. \tag{21}$$

The hydraulic power $P_h$ and the pump torque can be described, respectively.

$$P_h = \rho g H \tag{22}$$

$$T_p = k_r\omega_r^2 + T_s. \tag{23}$$

## 4 Proposed Design Procedure of Fuzzy-Based Control Strategy

The closed-loop voltage/frequency control method is characterized by its simplicity and good accuracy of motor speed. But, it is not applicable for systems requiring servoperformance or high response to large dynamic torque/speed changes. The proposed fuzzy-based PID control strategy constitutes two main tasks. The first task aims at estimating the motor speed while the second task emulates a closed-loop controller to preserve robust operation of the modified six-phase IM. Figure 3 shows the schematic diagram of the proposed closed-loop fuzzy-based control scheme for the six-phase IM.

### 4.1 Speed Estimation Procedure

The proposed speed estimator aims to evaluate the speed at economical costs and less complexity of the drive system. The estimation of the flux linkage of the machine, whatever the speed, is estimated as the procedure (Abdelwanis et al. 2015; Fatemi et al. 2014). Figure 4 shows the flowchart of the procedure of speed estimator on the basis of motor parameters and captured signals of motor parameters.

The d and q voltage components at the motor terminals of the stator side can be expressed as:

$$V_{qs} = R_s I_{qs} + p\lambda_{qs} - \omega\lambda_{ds} \quad (24)$$

$$V_{ds} = R_s I_{ds} + p\lambda_{ds} - \omega\lambda_{qs}. \quad (25)$$

The flux derivative component can be computed from,

$$\lambda'_{dr} = \left[\frac{L_r}{L_m}(V_{ds} - I_{ds})R_s + \sigma L_s S\right] \quad (26)$$

$$\lambda'_{qr} = \left[\frac{L_r}{L_m}\left(V_{qs} - I_{qs}\right)R_s + \sigma L_s S\right] \quad (27)$$

The flux component can be computed from,

$$\lambda_{qr} = p\left(\dot{\lambda}'_{qr}\right) \quad (28)$$

$$\lambda_{dr} = p(\dot{\lambda}'_{dr})\,. \quad (29)$$

The estimated speed can be calculated from,

$$\omega_r = \frac{1}{\widehat{\lambda}_r^2}\left[\left(\lambda_{dr}\lambda'_{qr} - \lambda_{qr}\lambda'_{dr}\right) - \frac{L_m}{T_r}\left(\lambda_{dr}I_{qs} - \lambda_{qr}I_{ds}\right)\right] \quad (30)$$

where:

$$\sigma = 1 - \frac{L_m^2}{L_r L_s} \quad (31)$$

$$\widehat{\lambda}_r^2 = \lambda_{qr}^2 + \lambda_{dr}^2 \quad (32)$$

$$T_r = \frac{L_r}{R_r}. \quad (33)$$

### 4.2 Design of Closed-Loop Control System

To enhance the performance of system, a closed-loop V/f control was investigated. In the proposed method, the speed estimator of the motor is employed. The estimated motor speed is considered as the input signal of the closed-loop controller. The estimated speed is compared with the reference speed to obtain the error signal. The magnitude error signal and its sign can be calculated from the difference between the actual and reference values of the speed as:

$$e(t) = \omega_{ref} - \omega_r. \quad (34)$$

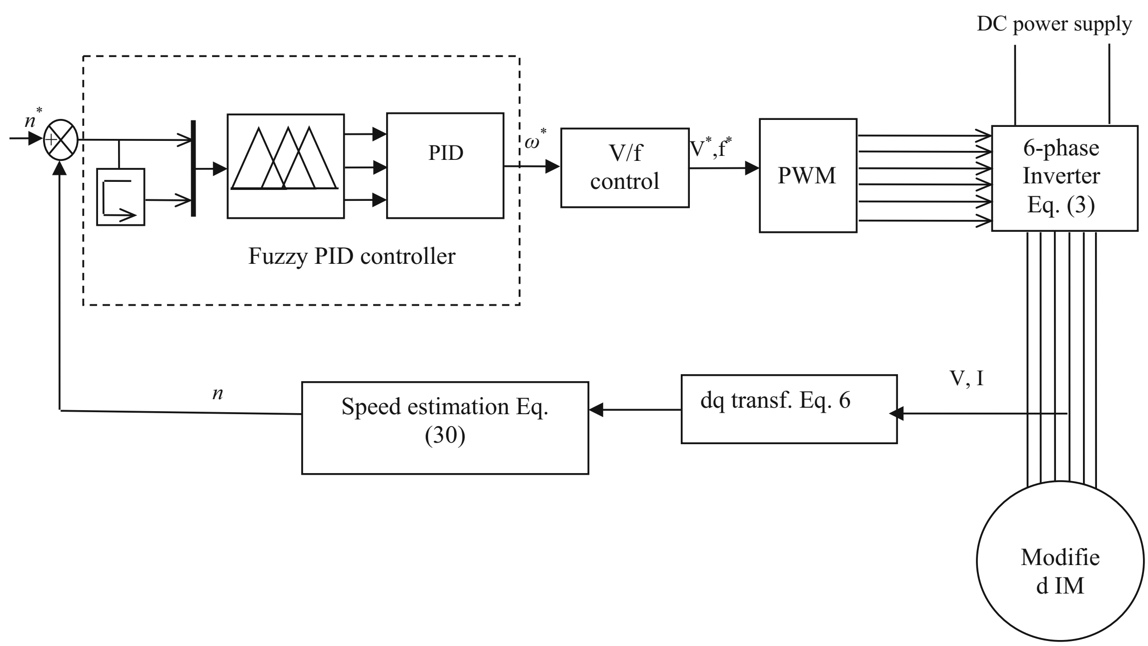


**Fig. 3** The schematic diagram of the proposed closed-loop control system with fuzzy PID controller

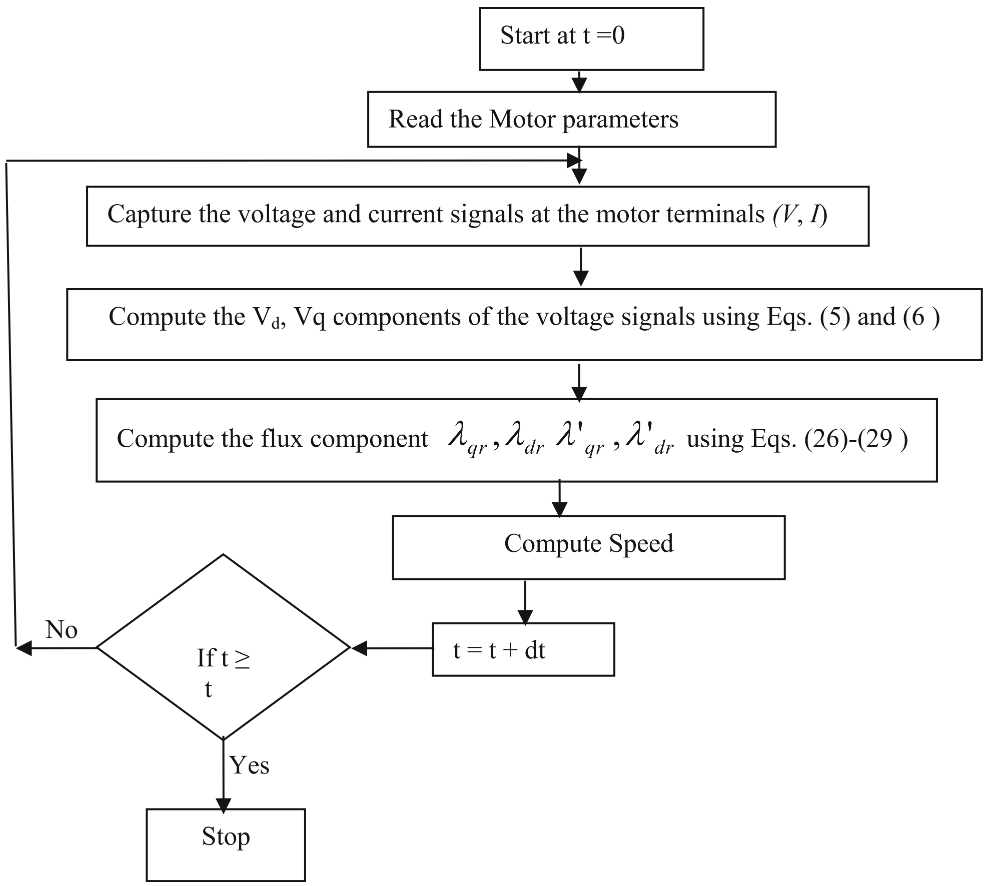


**Fig. 4** Flowchart of speed estimator

Based on the error of speed, the PID controller generates the corrected motor stator frequency deviation to compensate perfectly the raised error. In the V/f closed-loop control application, the feedback speed signal is obtained from the motor parameters, measuring the currents and voltages.The design of PID controller is required in order to determine the three coefficients: $K_p$, $K_i$, $K_d$.

$$u(t) = K_p e(t) + K_i \int e(t)\mathrm{d}t + K_d \frac{\mathrm{d}e(t)}{\mathrm{d}t} \tag{35}$$

where, $K_i = K_p/T_i$ and $K_d = K_p.\ T_d$ in which $T_i$ is the integral time constant and $T_d$ is derivative time constant. PID controller can be defined in Laplace form as:

$$G(s) = K_p\left(1 + \frac{1}{T_i s} + K_d s\right). \tag{36}$$

The PID is the primary controller and fuzzy system as a secondary controller controls the PID parameters. Two signals called speed error and change of error is brought in the fuzzy block inputs and then resulting the tuned PID coefficients. The tuned PID leads to the control signal and delivers it to the inverter. According to Eqs. (37)–(43), the parameters $K_p$ and $K_d$ have been determined in the range of maximum and minimum from the tests. For convenience, by using the following relation of $K_p$ and $K_d$ they are normalized between 0 and 1:

$$K'_p = \left(\frac{K_p - K_{pmin}}{K_{pmax} - K_{pmin}}\right) \tag{37}$$

$$K'_d = \left(\frac{K_d - K_{dmin}}{K_{dmax} - K_{dmin}}\right) \tag{38}$$

$$T_i = \alpha T_d \tag{39}$$

$$K_i = \frac{K_p}{\alpha T_d} = \frac{K_p^2}{\alpha K_d}. \tag{40}$$

The fuzzy inputs are $e(t)$ and $\dot{e}(t)$ and the outputs are $K'$p, $K'$d, and $\alpha$. Then, fuzzified PID coefficients are modelled as:

$$K_p = \left(K_{pmax} - K_{pmin}\right)K'_p + K_{pmin} \tag{41}$$

$$K_d = \left(K_{dmax} - K_{dmin}\right)K'_d + K_{dmin} \tag{42}$$

$$K_i = \frac{K_p^2}{\alpha K_d}. \tag{43}$$

Figure 5 shows the fuzzy-based procedure for the PID parameters to obtain the robust control signal.

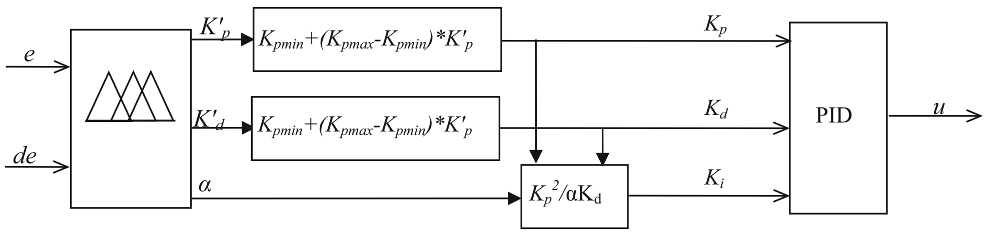


**Fig. 5** Fuzzy-based tuning of PID coefficients

### 4.3 Fuzzy PID Parameters

The variables $e(t)$ and $de(t)$ are modelled in the fuzzy environment to fuzzy variables. The fuzzy membership functions are developed for input and output variables in fuzzy domain that have been chosen as shown in Figs. 6 and 7. The universe of discourse of all the input is divided into seven overlying fuzzy sets. The operation range of all the output ($K_p$, $K_d$) is chosen as shown in Fig. 7. Each universe of discourse is divided into two overlapped fuzzy sets. The universe of discourse of the output ($\alpha$) is established by four overlapping fuzzy sets. Each fuzzy variable has degree of membership ($\mu$). The membership degree belongs to the range [0, 1]. The rule bases for three fuzzy parameter tuners, e.g. $k_p$, $k_d$, and $\alpha$, are shown in Table 1.

## 5 Applications

### 5.1 Simulated Cases

To carry out the proposed procedure for speed estimator, the MATLAB/Simulink is adopted for modelling the combined modified three-phase induction motor to work as six-phase IM-pumping system. Four studied cases can be classified as shown in Table 2 to simulate sequential operating condition. The speed controller is working with the aid of the proposed fuzzy PID mechanism. The six-phase IM parameters are recorded in Table 3.

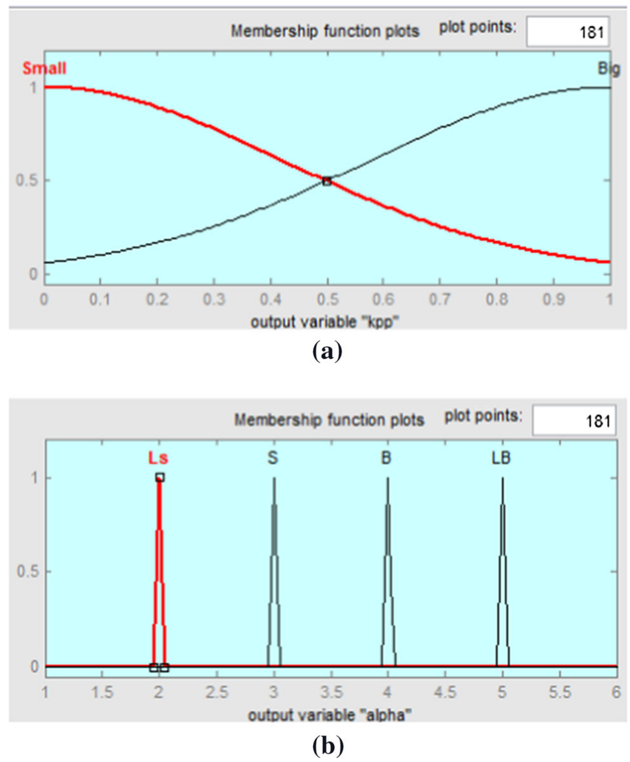


**Fig. 7** Output membership functions of $K_p$, $K_d$, and $\alpha$. **a** Membership of $K_p$, and $K_d$, **b** output membership functions of $\alpha$. Note: S (small), B (big), LS (large small), and LB (large big)

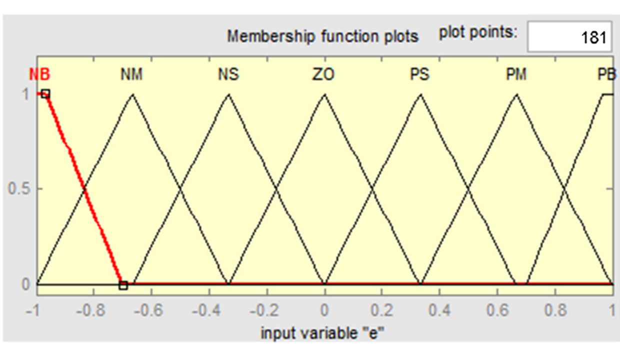


**Fig. 6** Input membership functions for error and change of error. Note: NB (negative big), NM (negative medium), NS (negative small), ZO (zero), PS (positive small), PM (positive medium), and PB (positive big)

### 5.2 Simulation Results

Figure 8 shows the speed variation for conventional PID (CPID) and fuzzy PID (FPID) controllers. It has cleared the effectiveness of the estimation procedure to identify the motor speed. The speed for both cases is close to the actual speed. The FPID controller has better performance in terms of the rise time and steady-state error. Figure 9 shows the pumping torque variation for the four studied cases. The closeness between the estimated senseless speeds with actual mechanical speed was clear. The total harmonic

**Table 1** Truth Table of fuzzy rules of the proposed fuzzy PID controller

| *e* | de | $k_p$ | $k_d$ | *A* | *e* | de | $K_p$ | $K_d$ | α |
|---|---|---|---|---|---|---|---|---|---|
| NB, PB | NB | B | S | LS | NS, PS | NB | S | B | B |
| | NM | B | S | LS | | NM | S | B | S |
| | NS | B | S | LS | | NS | B | B | S |
| | ZO | B | S | LS | | ZO | B | S | LS |
| | PS | B | S | LS | | PS | B | B | S |
| | PM | B | S | LS | | PM | S | B | S |
| | PB | B | S | LS | | PB | S | B | B |
| NM, PM | NB | S | B | S | ZO | NB | S | B | LB |
| | NM | B | B | S | | NM | S | B | B |
| | NS | B | S | LS | | NS | S | B | S |
| | ZO | B | S | LS | | ZO | B | B | S |
| | PS | B | S | LS | | PS | S | B | S |
| | PM | B | B | S | | PM | S | B | B |
| | PB | B | B | S | | PB | S | B | LB |

**Table 2** Sequence of six-phase IM-pumping system operation with fuzzy PID controller

| Case no. | Period (min) | | Description |
|---|---|---|---|
| | From | To | |
| 1 | 0 | 0.5 | Starting period |
| 2 | 0.5 | 1.5 | Normal operation (normal speed) |
| 3 | 1.5 | 2.5 | Operating condition (reduced speed) |
| 4 | 2.5 | 3 | Return to normal operating condition |

distortions for voltage and current are presented in Figs. 10 and 11, respectively. Figure 12 represents the applied voltage–time characteristics for the studied cases. Figure 13 shows clearly that the stator current in the first period increases rapidly to its maximum value at the starting instant. It was reduced to its rated value in the

**Table 3** Six-phase induction motor parameters

| Parameters | Values | Parameters | Values |
|---|---|---|---|
| $L_{ls}$ (*H*) | 0.013 | $R_r$ Ω | 0.9 |
| $L_m$ (*H*) | 1 | *J kg* $m^2$ | 0.02 |
| $L_{lr}$ (*H*) | 0.013 | *P* | 2 |
| $R_s$ Ω | 2 | $V_{ph}$ *V* | 220 |

second period (Case 2). The torque speed characteristics for motor and pump at 2800 and 2000 rpm are presented in Fig. 14.

Figure 15 shows that $K_p$ is tracking with speed change as follows, in the second period 0.366, in third period it is increased to 0.3674, in the fourth period it is 0.367, $K_i$ decreases with speed decrease, in the second period it is 0.0851, in the third period it increased to 0.082, in the fourth period it is 0.0848, and $K_d$ increases with speed decrease, in the second period it is 0.0042, in the third

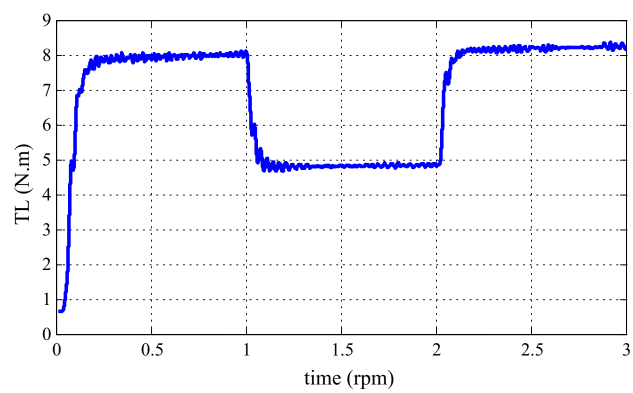


**Fig. 9** Pump torque–time characteristics with fuzzy PID

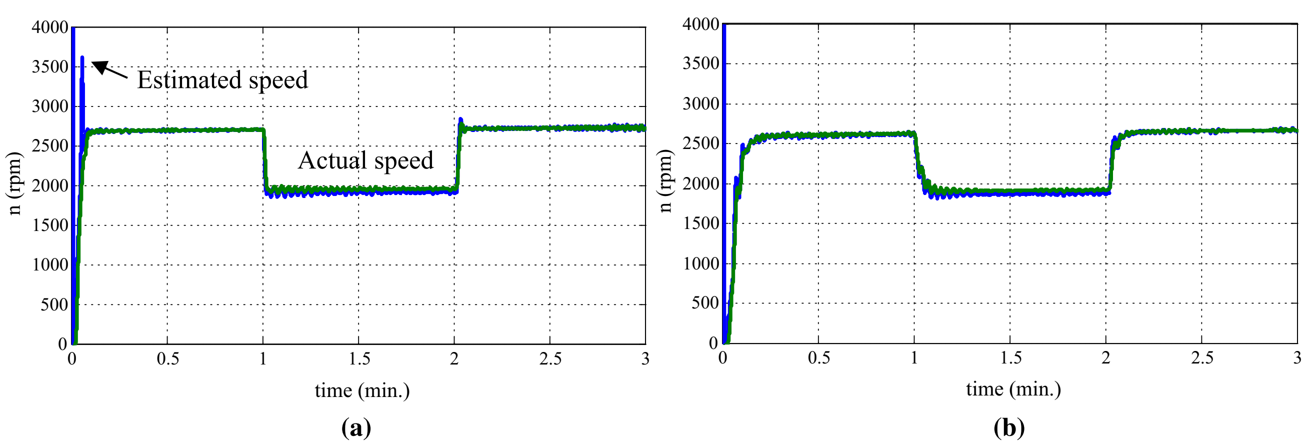


**Fig. 8** Estimated and actual speed–time characteristics for PID controllers. **a** PID, **b** fuzzy PID

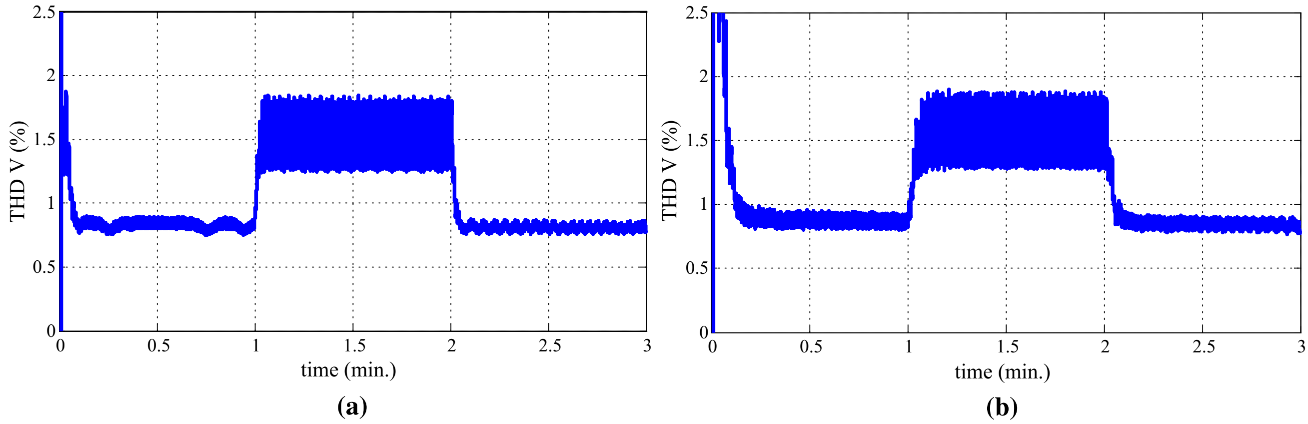


**Fig. 10** THD in voltage–time characteristics for PID controllers. **a** With PID, **b** fuzzy PID

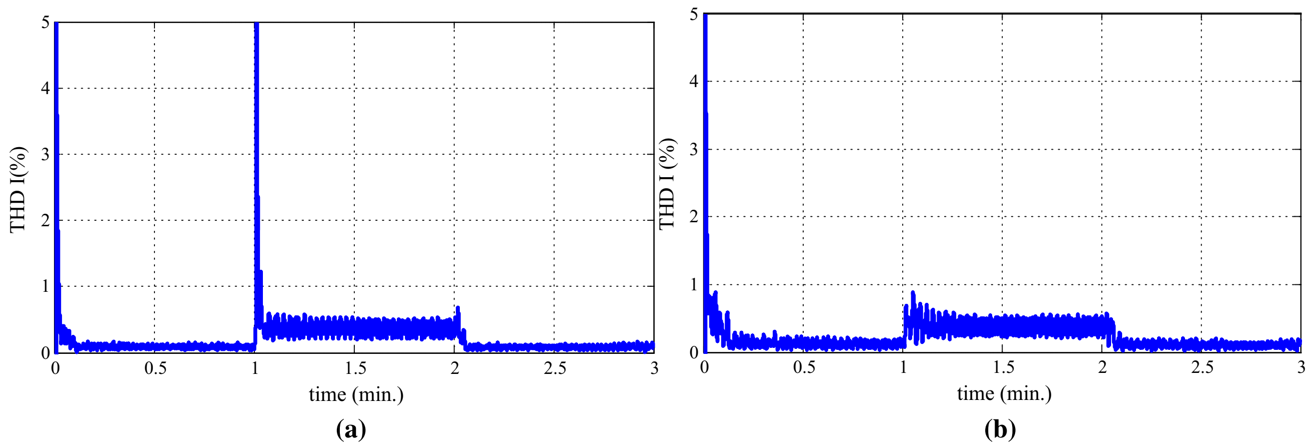


**Fig. 11** THD in current–time characteristics for PID controllers. **a** With PID, **b** fuzzy PID

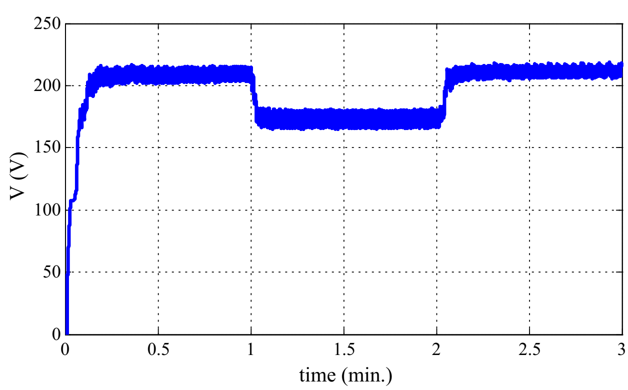


**Fig. 12** Applied voltage–time characteristics with fuzzy PID

period it increased to 0.00,435, and in the fourth period it is 0.0043.

Table 4 shows an assessment study for the proposed fuzzy PID (FPID) controller compared with the conventional PID (CPID) controller, which is based on trial and error. From this table, the following benefits of fuzzy PID controller can be summarized, compared with the conventional one:

(1) The use of FPID controller leads to decrease in the speed overshot and the corresponding steady-state error for cases 2–4.

(2) The current is reduced by 33, 25, and 15% for Case 2–4, respectively, with the proposed FPID controller.

(3) The highest total harmonic distortion levels of current signal for cases 2–4 are 4.8, 0.9, and 0.28%. These $THD_I$ levels are located within the permissible harmonic limitations.

(4) The estimated speed using the proposed estimation procedure is very close to the actual speed for all studied cases, while the conventional estimator is far from the true speed with errors reaching to 5–30% for different case studies.

(5) The proposed FPID improves the rise time compared with CPID controllers in the range 2.5–25%.

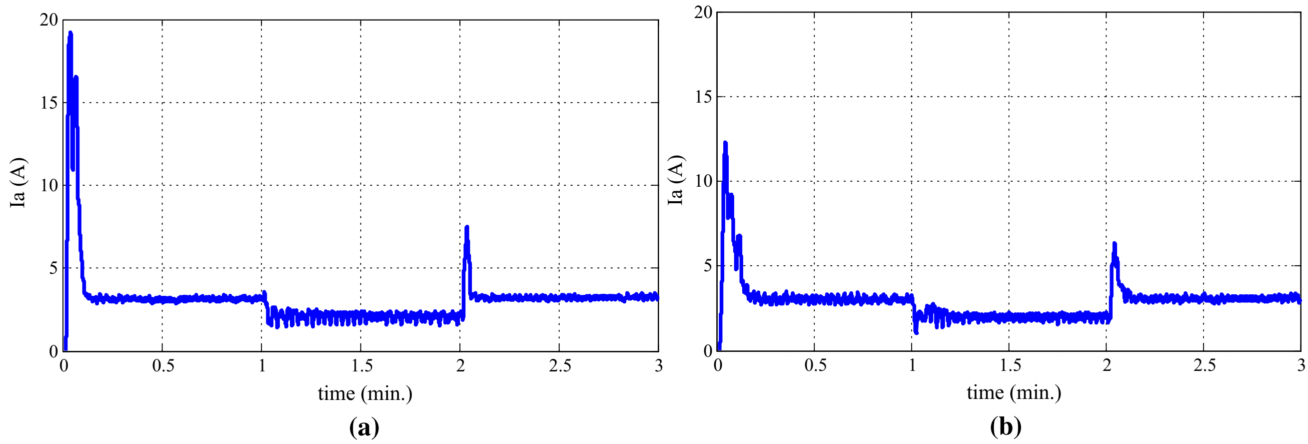


Fig. 13 Stator phase current–time characteristics. **a** With PID, **b** fuzzy PID

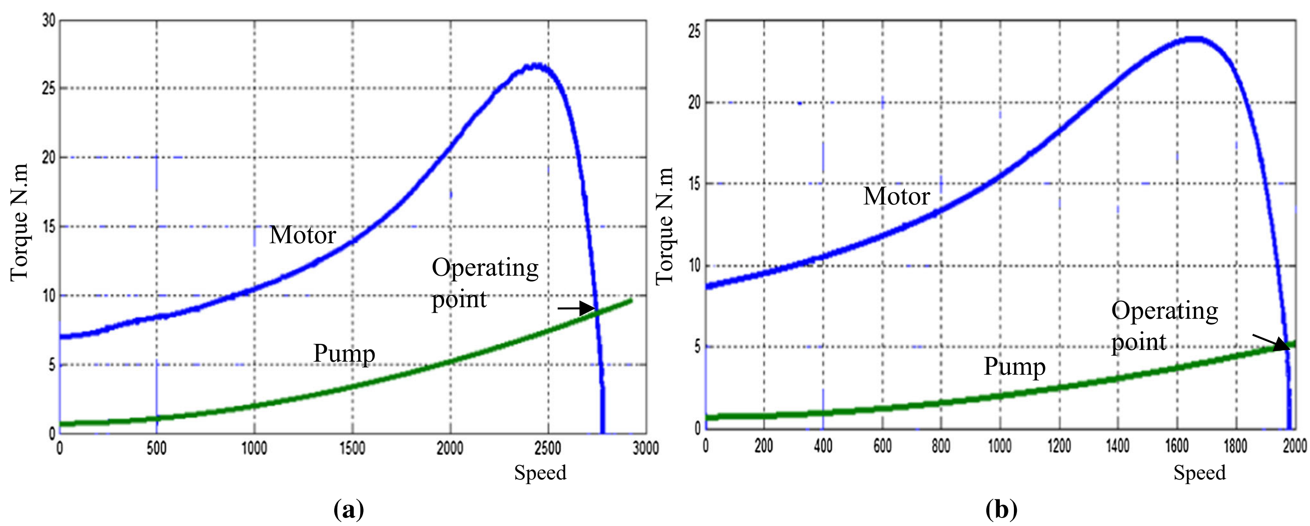


Fig. 14 Torque–speed characteristics for motor and pump with fuzzy PID. **a** Torque–speed characteristics at 2800 rpm, **b** torque–speed characteristics at 2000 rpm

## 6 Conclusions

This study has presented the implementation and detailed analysis study of the six-phase IM that drives a centrifugal pump system. A fuzzy-based tuning scheme of PID coefficients has been proposed to sustain the motor speed at the predefined reference values. The obtained fuzzy-based tuned parameters were compared with conventional PID. The PID controllers have been accomplished with a scalar V/f closed-loop six-phase IM. The results show that the PWM inverter reduces the THD for current and voltage waveforms. It is clear that the performance of the modified six-phase IM is enhanced compared with the equivalent three-phase induction motor. It was observed that the proposed modification enhances torque pulsation and the motor reliability. The following benefits of fuzzy PID controller compared with the conventional one can be summarized as:

(1) The use of fuzzy PID controller leads to decrease in the speed overshot and steady-state error for the studied cases.
(2) The current is reduced by 15–33% for the studied cases with the proposed fuzzy-based PID controller.
(3) The highest total harmonic distortion levels of current signal are located within the permissible harmonic limitations.

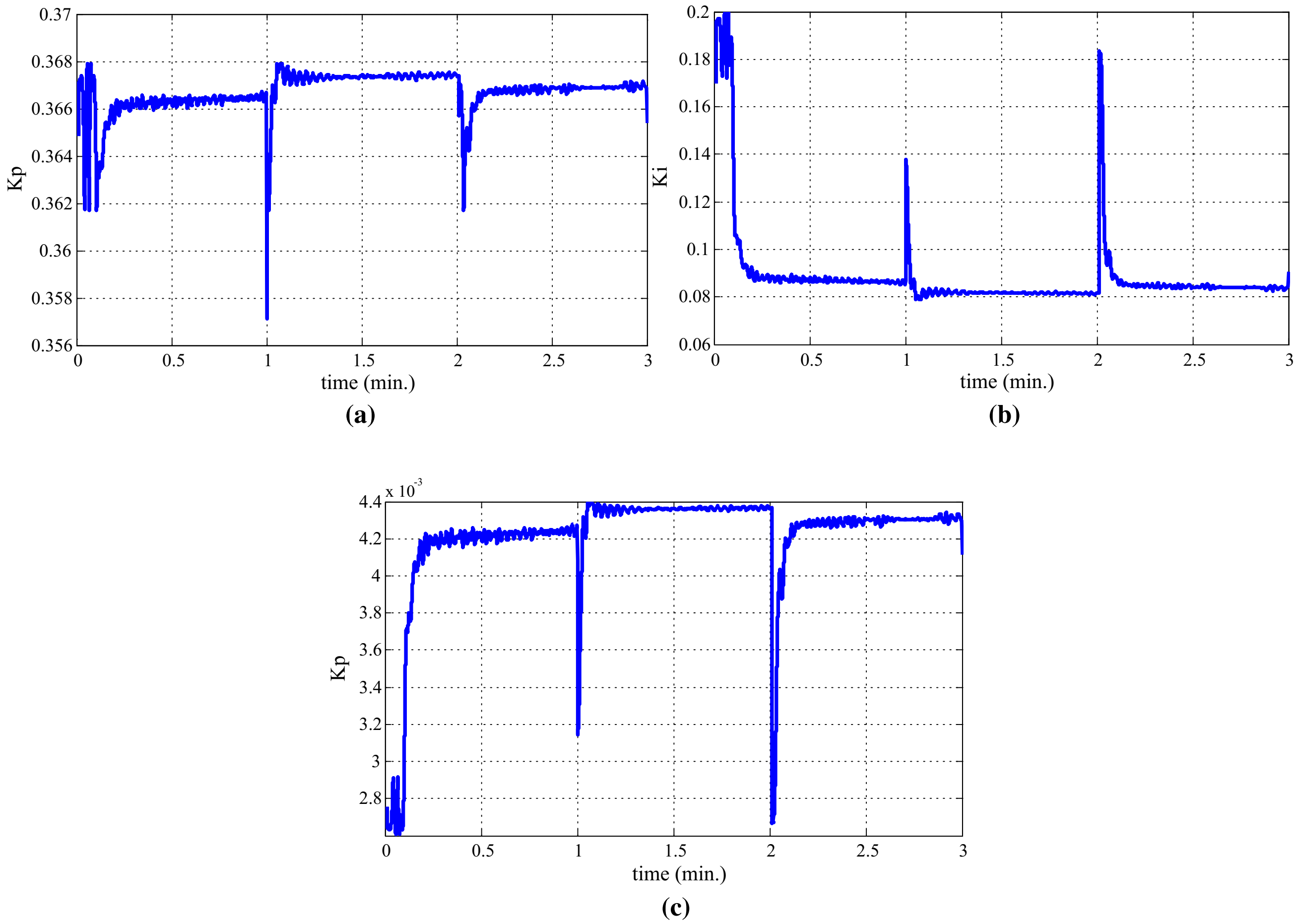


**Fig. 15** Tuned fuzzy parameters ($K_p$, $K_i$, and $K_d$) of PID control **a** $K_p$, **b** $K_i$, **c** $K_d$

**Table 4** Assessment of fuzzy PID against conventional PID controllers

| Index | Controller | Case 2 | | Case 3 | | Case 4 | |
|---|---|---|---|---|---|---|---|
| | | Overshot | Steady-state error | Overshot | Steady-state error | Overshot | Steady-state error |
| Speed (rpm) | CPID | 2712 | 33 | 1989 | 88 | 2780 | 53 |
| | FPID | 2645 | 30 | 1960 | 30 | 2692 | 30 |
| Current (A) | CPID | 19.2 | 0.5 | 3.6 | 0.8 | 7.5 | 0.35 |
| | FPID | 12.3 | 0.5 | 2.7 | 0.5 | 6.4 | 0.35 |
| THD I (%) | CPID | 18.3 | 0.1 | 15.2 | 0.35 | 0.68 | 0.08 |
| | FPID | 4.8 | 0.15 | 0.9 | 0.25 | 0.28 | 0.12 |
| Estimated speed (rpm) | CPID | 3615 | 35 | 1976 | 65 | 2839 | 45 |
| | FPID | 2647 | 30 | 1950 | 25 | 2689 | 35 |
| Rise time (min.) | CPID | 0.08 | | 0.08 | | 0.08 | |
| | FPID | 0.078 | | 0.07 | | 0.06 | |

(4) The estimated speed using the proposed estimation procedure is very close to the actual speed for all studied cases. While the conventional estimator is far from the true speed with errors reaching to 5–30% for different case studies.

(5) The proposed fuzzy PID improves the rise time compared with conventional PID controllers in the range 2.5–25%.

(6) Evaluation of the motor performance is analysed for a wide range of operating loading conditions.

## References


Abdelwanis MI, Selim F (2015) A sensorless controller of submersible motors fed from photovoltaic system. In: 17th international middle-east power system conference (MEPCON'15) Mansoura University, Egypt, December 15–17

Abdelwanis MI, Selim F, El-Sehiemy RAA (2015) An efficient sensorless slip dependent thermal motor protection schemes applied to submersible pumps. Int J Eng Res Afr 14:75–86

Abou E-E, Sehiemy RA, Shaheen AM (2010) Multi-objective fuzzy based procedure for optimal reactive power dispatch problem. In: Proceedings 14th international middle east power systems conference (MEPCON'10), Cairo University, Egypt, pp 941–946

Azeddine B, Ghalem B (2010) Six-phase matrix converter fed double star induction motor. Acta Polytech Hung 7(3):163–176

Barrero F, Duran MJ (2016a) Recent advances in the design, modeling, and control of multiphase machines—part I. IEEE Trans Ind Electron 63(1):449–458

Barrero F, Duran MJ (2016b) Recent advances in the design, modeling and control of multiphase machines—part 2. IEEE Trans Ind Electron 63(1):459–468

El Sehiemy RA, El-Ela AAA, Shaheen AAM (2013) Multi-objective fuzzy-based procedure for enhancing reactive power management. IET Gener Transm Distrib 7(12):1453–1460

El Sehiemy RA et al (2015) A multi-objective fuzzy-based procedure for reactive power-based preventive emergency strategy. Int J Eng Res Afr 13:91–102

El-Ela AAA, Bishr M, Allam S, El-Sehiemy R (2005) Optimal preventive control actions using multi-objective fuzzy linear programming technique. Electr Power Syst Res 74(1):147–155

Elhosseini MA, El Sehiemy RA, Salah AH, Abido MA (2017) Modelling and control of an interconnected combined cycle gas turbine using fuzzy and ANFIS controllers. Electr Eng 100(2):763–785. https://doi.org/10.1007/s00202-017-0547-x

El-Sehiemy RA, Aleem SHA, Abdelaziz AY, Balci ME (2017) A new fuzzy framework for the optimal placement of phasor measurement units under normal and abnormal conditions. Resour Effic Technol 3:542–549

Fatemi SMJR, Abjadi NR, Soltani J, Abazari S (2014) Speed sensorless control of a six-phase induction motor drive using backstepping control. IET Power Electron 7(1):114–123

Fnaiech MA, Betin F, Capolino G-A, Fnaiech F (2010) Fuzzy logic and sliding-mode controls applied to six-phase induction machine with open phases. IEEE Trans Ind Electron 57(1):354–364

Gautam A, Ojo O, Ramezani M, Momoh O (2012) Computation of equivalent circuit parameters of nine-phase induction motor in different operating modes. In: Energy conversion congress and exposition (ECCE), 2012 IEEE, IEEE, pp 142–149

Han WY, Kim SM, Kim SJ, Lee CG (2003) Sensorless vector control of induction motor using improved self-tuning fuzzy PID controller. In: SICE 2003 annual conference, vol 3, IEEE. pp 3112–3117)

Ho TJ, Yeh LY (2010) Design of a hybrid PID plus fuzzy controller for speed control of induction motors. In: 2010 the 5th IEEE conference on industrial electronics and applications (ICIEA). IEEE, pp 1352–1357

Huang J, Kang M, Yang J, Jiang H, Liu D (2008) Multiphase machine theory and its applications. In: International conference on electrical machines and systems, 2008. ICEMS 2008, IEEE, pp 1–7

Kang M, Huang J, Yang J, Liu D, Jiang H (2009) Strategies for the fault-tolerant current control of a multiphase machine under open phase conditions. In: International conference on electrical machines and systems, 2009. ICEMS 2009, IEEE, pp 1–6

Kiani-Nezhad R, Nahidmobarakeh B, Baghli L, Betin F, Capolino GA (2008) Modeling and control of six-phase symmetrical induction machines under fault condition due to open phases. IEEE Trans Ind Electron 55(5):1966–1977

Kim Hyunbae, Harke Michael C, Lorenz Robert D (2003) Sensorless control of interior permanent-magnet machine drives with zero-phase lag position estimation. IEEE Trans Ind Appl 39(6):1726–1733

Kudinov YI, Kolesnikov VA, Pashchenko FF, Pashchenko AF, Papic L (2017) Optimization of fuzzy PID controller's parameters. Procedia Comput Sci 103:618–622

Kumar RA, Daya JF (2013) A novel self-tuning fuzzy based PID controller for speed control of induction motor drive. In: 2013 international conference on control communication and computing (ICCC). IEEE, pp 62–67

Kundrotas B, Lisauskas S, Rinkeviciene R (2011) Model of multiphase induction motor. Electron Electr Eng Kaunas Technol 111(5):111–114

Lega A, Mengoni M, Serra G, Tani A, Zarri L (2010) General theory of space vector modulation for five-phase inverters. In: IEEE xplore, March 19, pp 237–244

Levi E, Bojoi R, Profumo F, Toliyat HA, Williamson S (2007a) Multiphase induction motor drives–a technology status review. IET Electr Power Appl 1(4):489–516

Levi E et al (2007b) Multiphase induction motor drives-a technology status review. Electr Power Appl IET 1(4):489–516

Lyra ROC, Lipo TA (2002) Torque density improvement in a six-phase induction motor with third harmonic current injection. IEEE Trans Ind Appl 38(5):1351–1360

Mandal S (2015) Performance analysis of six-phase induction motor. Int J Eng Res Technol (IJERT) 4(02):589–593

Nabi HP, Dadashi P, Shoulaie A (2011) A novel structure for vector control of symmetrical six-phase induction machines with three current sensors. ETASR Eng Technol Appl Sci Res 1(2):23–29

Nagaraj P, Kannan V, Santhi M (2014) Modified multiphase induction motor with high starting torque. Int J Innov Res Sci Eng Technol 3(SI 3):519–522

Nanoty A, Chudasama AR (2012a) Testing of designed developed prototype six phase induction motor and analysis of problems faced in actual development. IOSR J Electr Electron Eng (IOSR-JEEE):1–6, e-ISSN: 2278-1676, p-ISSN: 2320-3331

Nanoty A, Chudasama AR (2012b) Control of designed developed six phase induction motor. Int J Electromagn Appl 2(5):77–84

Nanoty A, Chudasama AR (2013) Design, development of six phase squirrel cage induction motor and its comparative analysis with equivalent three phase squirrel cage induction motor using circle diagram. Int J Emerg Technol Adv Eng 3(8):731–737

Pant GKSV (2000) Analysis of a multiphase induction machine under fault condition in a phase-redundant AC drive system. Electr Mach Power Syst 28(6):577–590

Renukadevi G, Rajambal K (2012) Generalized d-q model of n-phase induction motor drive. Int J Electr Comput Electron Commun Eng 6(9):62–71

Renukadevi G, Rajambal K (2013) Modeling and analysis of multi-phase inverter fed induction motor drive with different phase numbers. WSEAS Trans Syst Control 8(3):73–80

Sculler F, Charpentier JF, Semail E, Clénet S (2006) A global design strategy for multiphase machine applied to the design of a 7-phase fractional slot concentrated winding PM machine. In: Proceedings of ICEM, vol 6

Singh GK (2002) Multi-phase induction machine drive research—a survey. Electr Power Syst Res 61(2):139–147

Sriram Pavan Kumar N, Kalyan Chakravarthi NS (2016) A novel structure for rotor flux and current control of a symmetrical six-phase induction machine. Int J Glob Innov 4(I):35–40

Taheri A, Rahmati A, Kaboli S (2012) Comparison of efficiency for different switching tables in six-phase induction motor DTC drive. J Power Electron 12(1):128–135

Xia JK, Min L, Liu K (2010) Fuzzy control scheme for vector-controlled multiphase induction motor drive. In: 2010 international conference on digital manufacturing and automation (ICDMA), vol 1. IEEE, pp 757–760

Xu J, Feng X, Mirafzal B, Demerdash NA (2006) Application of optimal fuzzy PID controller design: PI control for nonlinear induction motor. In: The Sixth World Congress on intelligent control and automation, 2006. WCICA 2006, vol 1. IEEE, pp 3953–3957

Yuanxi W, Yali Y, Guosheng Z, Xiaoliang S (2012) Fuzzy auto-adjust PID controller design of brushless DC motor. Phys Procedia 33:1533–1539

Zhao S, Yuan H (2011) Asynchronous motor vector control based on fuzzy adaptive PID controller. In: 2011 IEEE 3rd international conference on communication software and networks (ICCSN). IEEE, pp 677–679